Coherent and incoherent *d* band dispersions in $SrVO_3$

M. Takizawa,[1] M. Minohara,[2] H. Kumigashira,[3,4] D. Toyota,[3] M. Oshima,[2,3,4] H. Wadati,[1] T. Yoshida,[1] A. Fujimori,[1] M. Lippmaa,[5] M. Kawasaki,[6,4] H. Koinuma,[7] G. Sordi,[8] and M. Rozenberg[8]

[1]*Department of Physics, University of Tokyo, Bunkyo-ku, Tokyo 113-0033, Japan*

[2]*Graduate School of Arts and Sciences, University of Tokyo, 3-8-1 Komaba, Meguro-ku, Tokyo 153-8902, Japan*

[3]*Department of Applied Chemistry, University of Tokyo, Bunkyo-ku, Tokyo 113-8656, Japan*

[4]*Core Research for Evolutional Science and Technology, Japan Science and Technology Agency (JSTCREST), Chiyoda-ku, Tokyo 102-0075, Japan*

[5]*Institute for Solid State Physics, University of Tokyo, 5-1-5 Kashiwanoha, Kashiwashi, Chiba 277-8581, Japan*

[6]*Institute for Materials Research, Tohoku University, 2-1-1 Katahira, Aoba-ku, Sendai, Miyagi 980-8577, Japan*

[7]*Materials and Structures Laboratory, Tokyo Institute of Technology, 4259 Nagatsuta, Midori-ku, Yokohama, Kanagawa 226-8503, Japan*

[8]*Departamento de Física, FCEN, Universidad de Buenos Aires, Ciudad Universitaria Pabellón I, 1428 Buenos Aires, Argentina*

(Received 21 September 2009; revised manuscript received 3 November 2009; published 2 December 2009)

We have performed an angle-resolved photoemission spectroscopy study of $SrVO_3$ thin films. Utilizing thin films prepared *in situ*, with well-defined and atomically flat surfaces, contributions from surface states centered at ~ -1.5 eV were dramatically reduced, enabling us to study the bulklike V 3*d* states, including the incoherent part. A clear band dispersion is observed not only in the coherent part but also in the incoherent part and the spectral weight of the incoherent part is larger within the Fermi volume. These findings are particularly significant since the description of the so-called incoherent Hubbard band in $SrVO_3$ needs to include the nonlocal interaction between the atoms. These trends are well reproduced by dynamical mean-field theory calculations.

DOI: 10.1103/PhysRevB.80.235104 PACS number(s): 71.18.+y, 71.27.+a, 71.30.+h, 79.60.Dp

Metal-insulator transitions (MITs) in Mott-Hubbard systems have been extensively studied because of the fundamental importance in condensed-matter physics as well as the close relationship between MIT and remarkable phenomena such as high-temperature superconductivity in cuprates and colossal magnetoresistance in manganites.[1] Perovskite-type oxides ABO_3 are ideal systems to study bandwidth-control MIT because the bandwidth W can be controlled through the modification of the radius of the A-site ion and hence the B-O-B bond angle θ.[2–4] On the theoretical side, the recent development of dynamical mean-field theory (DMFT) has led to major progress in understanding MIT in strongly correlated systems.[5,6] According to DMFT, as U/W increases, where U is the on-site Coulomb energy, spectral weight is transferred from the coherent part, i.e., the quasiparticle band near the Fermi level (E_F), to the incoherent part or the so-called the Hubbard bands $\sim 1-2$ eV below E_F.[7]

The perovskite-type d^1 configuration material $Ca_{1-x}Sr_xVO_3$ (CSVO) is a typical bandwidth-controlled system, where the average A-site ionic radius and hence the bandwidth W can be continuously changed, although it remains metallic in the entire x range.[3] Extensive studies on CSVO have been made to understand the evolution of the electronic structure as a function of U/W, however the result has remained highly controversial until now. In an early photoemission spectroscopy (PES) study of CSVO, Inoue *et al.*[4] reported that as one decreases x in CSVO, i.e., increasing U/W, spectral weight is transferred from the coherent part to the incoherent part centered ~ 1.5 eV below E_F. By measuring the photon-energy-dependent PES of CSVO, Maiti *et al.*[8] have pointed out that surface states contribute to the incoherent part. Sekiyama *et al.*[9] have reported that using high-energy photons, i.e., in so-called "bulk-sensitive" PES, the spectral weight of the incoherent part is considerably reduced and that spectral weight transfer is not observed. Another bulk-sensitive PES study using very low-energy photons,[10] however, has indicated small differences between $SrVO_3$ (SVO) and $CaVO_3$ (CVO). Moreover, a PES study using polarized and unpolarized photons has indicated that matrix-element effect is important and that there is finite spectral weight transfer from the coherent part to the incoherent part in going from SVO to CVO.[11] A recent extended cluster-model analysis of the PES spectra has suggested that the reduction in spectral weight of the incoherent part at high photon energies is partly due to the effect of atomic-orbital cross sections.[12] In contrast to the controversial results mentioned above, a recent angle-resolved photoemission spectroscopy (ARPES) study by Yoshida *et al.*[13] has given clear-cut information about the coherent part near E_F. They successfully performed an ARPES study of cleaved bulk SVO crystals and observed the band dispersions of the coherent part.[13] However, the incoherent part seems to be dominated by surface states. Also, signals in the coherent part are too broad and weak to address issues of current interest such as the kink in dispersion, which recent DMFT calculations have predicted.[14,15]

In the present work, we have fabricated SVO thin films having high-quality atomically flat surfaces using the pulsed laser deposition (PLD) technique and studied the electronic structure by *in situ* ARPES measurements in far greater detail than has been possible before. ARPES experiments on thin films prepared *in situ* have recently turned out to have many advantages because the well-defined atomically flat surface enables us to obtain much more detailed ARPES spectra.[16,17] Such high-quality samples dramatically reduce the contribution of surface states and intrinsic dispersion behavior can be studied.

The PES measurements were performed at the soft x-ray

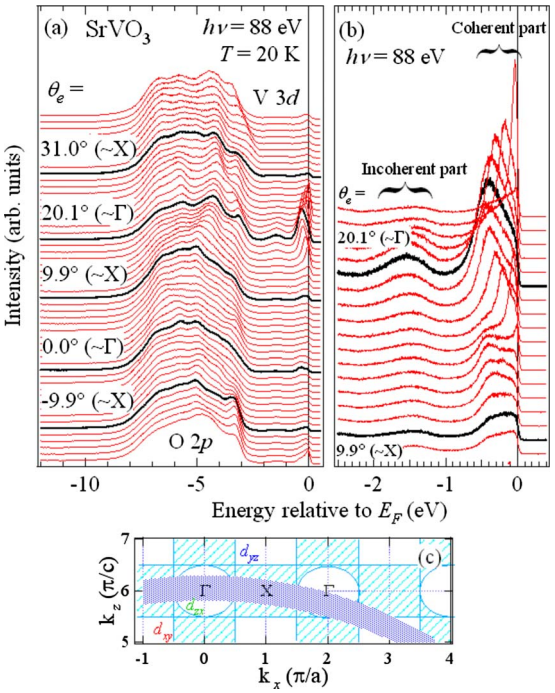

FIG. 1. (Color online) EDCs of $SrVO_3$ thin films. (a) Entire valence-band region. (b) Near the Fermi level. (c) Traces in k space including the uncertainties in the k_z direction. Schematic Fermi surfaces of $SrVO_3$ (junglegymlike mutually penetrating cylinders) are indicated by shaded area.

beamline BL-2C, the vacuum-ultraviolet (VUV) bend magnet beamline BL-1C and, the VUV undulator beamline BL-28B of photon factory (PF), High Energy Accelerators Research Organization (KEK), using a combined laser molecular-beam epitaxy-photoemission spectrometer system. Details of the experimental setup are described in Ref. 18. Epitaxial thin films of SVO were grown on single-crystal TiO_2-terminated Nb-doped $SrTiO_3$ substrates[19] by PLD. Films were deposited at 900 °C under a high vacuum of $\sim 10^{-8}$ Torr. The surface morphology of the measured SVO thin films was checked by *ex situ* atomic force microscopy, showing atomically flat step-and-terrace structures. The crystal structure was characterized by four-circle x-ray diffraction, confirming coherent growth on the substrate. The in-plane lattice constant was $a=3.905$ Å, the same as that of $SrTiO_3$ while the out-of-plane lattice constant was $c=3.82$ Å. Low-energy electron-diffraction patterns showed sharp 1×1 spots, with some superstructure spots of $\sqrt{2}\times\sqrt{2}$. There were two components in both the V $2p$ and the O $1s$ core-level spectra (not shown), indicating that the V^{5+}-oxide layer covered the surface of the thin films.[20] All PES measurements were performed in an ultrahigh vacuum of $\sim 10^{-10}$ Torr at 20 K using a Scienta SES-100 electron-energy analyzer. The total-energy resolution was set to about 30 and 150 meV for the spectra near E_F (BL-28B) and in the entire valence-band region (BL-1C), respectively.

A series of energy distribution curves (EDCs) taken at 88 eV with changing emission angles θ_e are shown in Figs. 1(a) and 1(b). The corresponding trace in k space is shown in Fig. 1(c). Here, the work function of the sample $\phi=4.5$ eV and the inner potential $V_0=11$ eV have been used to obtain the momentum k_z perpendicular to the surface, assuming free-electron final states. Although k_z is dependent on θ_e to some extent, as shown in Fig. 1(c), the ARPES spectra taken at 88 eV can be considered to trace the band in the Γ-X direction since band dispersions along high-symmetry lines are emphasized due to the finite width of k_z and the high k_x, k_y-resolved density of states around the high-symmetry lines.[21] For simplicity, we have also assumed a cubic Brillouin zone, although the unit cell of SVO thin films has a slight tetragonal distortion ($c/a\simeq 0.978$) due to epitaxial strain. Figure 1(a) shows clear dispersions both in the O $2p$ and V $3d$ bands. The bands between −10 and −3 eV are mainly composed of O $2p$ states while those between −3 eV to E_F belong mainly of V $3d$ states. In the V $3d$ band [Fig. 1(b)], there are two features: the coherent quasiparticle band near E_F and the incoherent part, which is also regarded as the lower Hubbard band. As previously reported,[13] the coherent part shows a clear dispersion. As for the incoherent part, there is a weak but finite dispersion as we shall describe below. It should be noted that the coherent peak is much sharper and more intense than in earlier work[13] owing to the high surface quality of the thin films. The relative intensity of the coherent part is very high when compared to the incoherent part. It has been recognized that the surface states appear around −1.5 eV and overlap the incoherent part of the PES spectra[8,9] and the intensity ratio of the coherent part to the incoherent part is similar to the "bulk" spectra reported in Refs. 8, 9, and 11. Thus we consider that the contributions from surface states seen in the previous work[8,9] were strongly reduced in the present SVO thin films. From the presence of the $\sqrt{2}\times\sqrt{2}$ surface reconstruction and the V^{5+} component in the V $2p$ core-level spectra described above, we infer that the V^{5+}-oxide capping layer, which has no electronic states within ~2 eV of E_F, protects the surface of SVO and hence the V $3d$ bands survive as in the bulk states within the band gap of the V^{5+} (d^0) oxide surface layer, as in the case of the $SrTiO_3$ capped $LaTiO_3$.[22]

In order to see the band dispersions more clearly, we have taken the second derivatives of the EDCs and displayed them in a false-color plot in Fig. 2. Although the obtained band structures qualitatively agree with local-density approximation (LDA) calculation (left-hand side of Fig. 2),[14,23,24] the position of the O $2p$ bands does not. Therefore, we have performed tight-binding (TB) band calculation to adjust the O $2p$ band position.[21] As shown in the right-hand side of Fig. 2, good agreement was obtained between experiment and calculation when the parameters were set as follows: $\epsilon_d-\epsilon_p=4.2$ eV, $\epsilon_{d\sigma}-\epsilon_{d\pi}=2.3$ eV, $\epsilon_{p\sigma}-\epsilon_{p\pi}=0.7$ eV, $(pd\sigma)=-2.2$ eV, $(pd\pi)=1.4$ eV, $(pp\sigma)=0.4$ eV, and $(pp\pi)=0$ eV. This was also confirmed by comparing the calculation with experiment along the X–M line obtained using $h\nu=60$ eV (not shown). Some of the bands, especially those in the dispersionless O $2p$ band around −7 eV, which cannot be reproduced by the calculation would be attributed to the $\sqrt{2}\times\sqrt{2}$ surface reconstruction. Taking into account the diffraction replica with respect to the $\sqrt{2}\times\sqrt{2}$ surface superstructure, almost all the experimental O $2p$ bands are well reproduced by the calculation (dashed curves in Fig. 2).

In order to see the V $3d$ bands near E_F in more detail, we

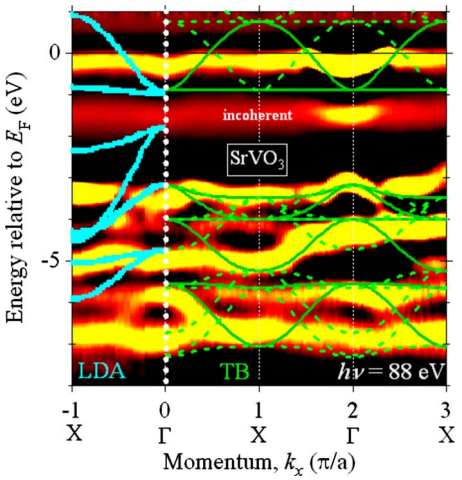

FIG. 2. (Color online) Experimental band structure deduced from the second derivative of EDCs, with bright parts corresponding to energy bands. LDA calculations from Ref. 23 and the fitted TB bands are shown by solid curves in the momentum range from $k_x=-\pi/a$ to 0 and from $k_x=0$ to $3\pi/a$, respectively. As for the TB bands, the diffraction replicas due to the $\sqrt{2}\times\sqrt{2}$ surface superstructure are also shown by dashed curves.

show in Fig. 3(a) the E-k_x space intensity plot along the Γ-X direction. The peak positions determined from both EDCs and momentum distribution curves (MDCs) are also shown. Between the Γ and X points, the degenerate V $3d_{xy}$ and $3d_{zx}$ bands cross the Fermi level while the dispersionless V $3d_{yz}$ band does not. One can see clear mass renormalization compared with the LDA calculation. From the experimental $(-0.44\pm0.02$ eV) and calculated (−0.95 eV) occupied bandwidths, the global mass-renormalization factor is estimated to be ~2. That is, as shown in Fig. 3(a), if the LDA band dispersions (light solid thick curves) are reduced by a factor of 0.5, the experimental band dispersions are well reproduced. This indicates that electron correlation strength is nearly independent of momentum and of the orbital component (d_{xy}, d_{yz}, or d_{zx}) of the degenerate t_{2g} band. The kink in the band dispersion is weak and broad, if it exists, but the curvature does indeed change sign at around ~−0.2 eV, as predicted by a recent DMFT calculation.[14]

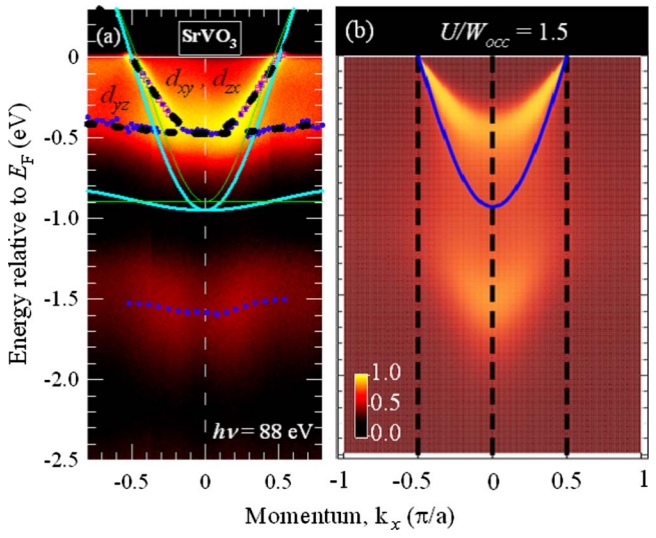

FIG. 3. (Color online) Energy-dependent and momentum-dependent spectral weight near the Fermi level (Ref. 25). (a) Experimental intensity plot for $SrVO_3$. Peak positions of the EDCs and MDCs are shown by filled circles and open squares, respectively. The V $3d$ bands from the LDA calculation and tight-binding calculation are also shown by solid thick and thin curves, respectively. Broken curves are LDA bands renormalized by a factor of 2. (b) Intensity plot of spectral function from DMFT calculation with $U/W_{occ}=1.5$, where $W_{occ}=0.4W$ is the width of the occupied part of the band.

As for the incoherent part located around −1.5 eV, one can see a weak but finite (~0.1 eV) dispersion and, significantly, a momentum dependence of the spectral intensity, with a maximum at the center of the Fermi volume (at the Γ point). In fact, this feature is clearly seen around the second Γ point, where the selection rules are relaxed (see Figs. 1 and 2) although the k_z momentum is slightly different from the Γ point. This is the experimental observation of the momentum-dependent electronic structure of an incoherent Hubbard band in a $3d$ transition-metal oxide. It would be interesting to see how the incoherent Hubbard band disperses in other Mott-Hubbard-type $3d$ transition-metal oxides, such as V_2O_3 and $La_{1-x}Sr_xTiO_3$.

Figure 3(b) shows the intensity plot of the spectral functions from the present DMFT calculation. In order to obtain the precise real frequency dependence of the spectral intensity, the DMFT self-energy was computed using the single band iterated perturbation theory, which for the occupied part of the density of states gives the same qualitative behavior as in the multiband case when there is one particle per unit cell. Agreement between experiment and theory is obtained when the correlation strength of U/W_{occ} is set to 1.5, where $W_{occ}=0.4W$ is the width of the occupied part of the noninteracting band. Although the DMFT calculation predicts that the incoherent part disperses as strongly as the bare band, the experimental dispersion of the incoherent part is considerably weaker than the DMFT prediction. This is probably due to the overlapping d_{yz} band which is dispersionless along the Γ-X direction, which has been neglected in the present DMFT calculation. Other effects may influence the weak dispersion of the incoherent part, such as the k_z momentum and the epitaxial strain of the thin film. Nevertheless is very significant the fact that DMFT correctly predicts that the maximum intensity of the Hubbard band occurs at the Γ point.

In conclusion, we have studied the electronic structure of $SrVO_3$ thin films by means of ARPES. Utilizing thin films with well-defined atomically flat surfaces, the bulklike V $3d$ band structure was successfully observed. The band dispersions in the coherent part were reproduced by the renormalized LDA bands with a global mass-renormalization factor of ~2. There was a weak but finite dispersion in the incoherent part and the intensity of the incoherent part was stronger within the Fermi volume. These finding are particularly significant since the description of the so-called incoherent Hubbard band in $SrVO_3$ needs to include the nonlocal interaction between the atoms. The experimental dispersions and intensities of the coherent part as well as of the incoherent part were well reproduced by momentum-resolved DMFT

calculation. Our experimental data for the incoherent band which are qualitatively well described by DMFT amount to the observation of the momentum-dependent electronic structure of the Hubbard band in transition-metal oxides.

The authors would like to thank K. Ono and A. Yagishita for their support in the experiment at KEK-PF and T. Mizokawa and K. Nasu for enlightening discussion. This work was supported by a Grant-in-Aid for Scientific Research (Grants No. A19204037, No. A19684010, and No. B19340094) from JSPS and a Grant-in-Aid for Scientific Research in Priority Areas "Invention of Anomalous Quantum Materials" from MEXT. Two of us (M.T. and H.W.) were supported by JSPS. The work was done under the approval of Photon Factory Program Advisory Committee (Proposals No. 2005G101 and No. 2005S2-002) at the Institute of Material Structure Science, KEK.

[1] M. Imada, A. Fujimori, and Y. Tokura, Rev. Mod. Phys. **70**, 1039 (1998).
[2] A. Fujimori, I. Hase, H. Namatame, Y. Fujishima, Y. Tokura, H. Eisaki, S. Uchida, K. Takegahara, and F. M. F. de Groot, Phys. Rev. Lett. **69**, 1796 (1992).
[3] I. H. Inoue, O. Goto, H. Makino, N. E. Hussey, and M. Ishikawa, Phys. Rev. B **58**, 4372 (1998).
[4] I. H. Inoue, I. Hase, Y. Aiura, A. Fujimori, Y. Haruyama, T. Maruyama, and Y. Nishihara, Phys. Rev. Lett. **74**, 2539 (1995).
[5] A. Georges, G. Kotliar, W. Krauth, and M. J. Rozenberg, Rev. Mod. Phys. **68**, 13 (1996).
[6] G. Sordi, A. Amaricci, and M. J. Rozenberg, Phys. Rev. Lett. **99**, 196403 (2007).
[7] X. Y. Zhang, M. J. Rozenberg, and G. Kotliar, Phys. Rev. Lett. **70**, 1666 (1993).
[8] K. Maiti, D. D. Sarma, M. J. Rozenberg, I. H. Inoue, H. Makino, O. Goto, M. Pedio, and R. Cimino, Europhys. Lett. **55**, 246 (2001).
[9] A. Sekiyama, H. Fujiwara, S. Imada, S. Suga, H. Eisaki, S. I. Uchida, K. Takegahara, H. Harima, Y. Saitoh, I. A. Nekrasov, G. Keller, D. E. Kondakov, A. V. Kozhevnikov, Th. Pruschke, K. Held, D. Vollhardt, and V. I. Anisimov, Phys. Rev. Lett. **93**, 156402 (2004).
[10] R. Eguchi, T. Kiss, S. Tsuda, T. Shimojima, T. Mizokami, T. Yokoya, A. Chainani, S. Shin, I. H. Inoue, T. Togashi, S. Watanabe, C. Q. Zhang, C. T. Chen, M. Arita, K. Shimada, H. Namatame, and M. Taniguchi, Phys. Rev. Lett. **96**, 076402 (2006).
[11] K. Maiti, U. Manju, S. Ray, P. Mahadevan, I. H. Inoue, C. Carbone, and D. D. Sarma, Phys. Rev. B **73**, 052508 (2006).
[12] R. J. O. Mossanek, M. Abbate, and A. Fujimori, Phys. Rev. B **74**, 155127 (2006).
[13] T. Yoshida, K. Tanaka, H. Yagi, A. Ino, H. Eisaki, A. Fujimori, and Z.-X. Shen, Phys. Rev. Lett. **95**, 146404 (2005).
[14] I. A. Nekrasov, K. Held, G. Keller, D. E. Kondakov, Th. Pruschke, M. Kollar, O. K. Andersen, V. I. Anisimov, and D. Vollhardt, Phys. Rev. B **73**, 155112 (2006).
[15] K. Byczuk, M. Kollar, K. Held, Y.-F. Yang, I. A. Nekrasov, Th. Pruschke, and D. Vollhardt, Nat. Phys. **3**, 168 (2007).
[16] A. Chikamatsu, H. Wadati, H. Kumigashira, M. Oshima, A. Fujimori, M. Lippmaa, K. Ono, M. Kawasaki, and H. Koinuma, Phys. Rev. B **76**, 201103(R) (2007).
[17] H. Wadati, A. Maniwa, A. Chikamatsu, I. Ohkubo, H. Kumigashira, M. Oshima, A. Fujimori, M. Lippmaa, M. Kawasaki, and H. Koinuma, Phys. Rev. Lett. **100**, 026402 (2008).
[18] K. Horiba, H. Oguchi, H. Kumigashira, M. Oshima, K. Ono, N. Nakagawa, M. Lippmaa, M. Kawasaki, and H. Koinuma, Rev. Sci. Instrum. **74**, 3406 (2003).
[19] M. Kawasaki, K. Takahashi, T. Maeda, R. Tsuchiya, M. Shinohara, O. Ishihara, T. Yonezawa, M. Yoshimoto, and H. Koinuma, Science **266**, 1540 (1994).
[20] Detailed characterization of this unique surface states using angle-dependent x-ray PES will be described elsewhere.
[21] H. Wadati, T. Yoshida, A. Chikamatsu, H. Kumigashira, M. Oshima, H. Eisaki, Z.-X. Shen, T. Mizokawa, and A. Fujimori, Phase Transitions **79**, 617 (2006).
[22] M. Takizawa, H. Wadati, K. Tanaka, M. Hashimoto, T. Yoshida, A. Fujimori, A. Chikamatsu, H. Kumigashira, M. Oshima, K. Shibuya, T. Mihara, T. Ohnishi, M. Lippmaa, M. Kawasaki, H. Koinuma, S. Okamoto, and A. J. Millis, Phys. Rev. Lett. **97**, 057601 (2006).
[23] K. Takegahara, J. Electron Spectrosc. Relat. Phenom. **66**, 303 (1994).
[24] E. Pavarini, A. Yamasaki, J. Nuss, and O. K. Andersen, New J. Phys. **7**, 188 (2005).
[25] Here, the simplified dispersion of a cubic t_{2g} band were assumed as in Ref. 24: $\varepsilon_{x_i x_j}(\mathbf{k}) = \epsilon_{t_{2g}} + 2t_\pi[\cos(k_{x_i}) + \cos(k_{x_j})] + 2t_\delta \cos(k_{x_k}) + 4t'_\sigma \cos(k_{x_i})\cos(k_{x_j})$, where $\epsilon_{t_{2g}} = 625$ meV, $t_\pi = -281$ meV, $t_\delta = -33$ meV, and $t'_\sigma = -96$ meV. In order to display the incoherent part visibly, the intensity has been modified using a hyperbolic tangent function.